https://doi.org/10.5194/ar-2026-15
Preprint. Discussion started: 13 April 2026

AEROSOL Research Discussions

Dispersion normalisation method for improved long-term trend evaluation: Heavy Metals in ambient air in the Czech Republic, Central Europe (2010–2021)

Adéla Holubová Šmejkalová[1], Radek Lhotka[1], Hana Škáchová[1], Jan Pacner[1]

[1]Air Quality Division, Czech Hydrometeorological Institute, Prague, 143 06, Czech Republic

Correspondence to: Adéla Holubová Šmejkalová (adela.holubova@chmi.cz)

Abstract. Long-term trends in atmospheric concentrations of heavy metals subject to legislative immission limits - Arsenic (6.0 ng m^{-3}), Cadmium (5.0 ng m^{-3}), Lead (500 ng m^{-3}), and Nickel (20 ng m^{-3}) - were evaluated at selected monitoring stations representing different environmental settings across the Czech Republic (in Central Europe) over twelve years. The dispersion normalisation method, which suppresses the influence of meteorological conditions on observed heavy metal concentrations, was employed to assess the effectiveness of legislative emission control measures. The results demonstrate statistically significant decreasing trends ($p < 0.001$) across all station types and all monitored heavy metals, except for Nickel at industrial stations, where no significant trend was detected. Furthermore, the systematic differences between original and dispersion-normalised concentration data confirm that meteorological variability can, in some cases, mask true emission levels, potentially leading to misinterpretation of air quality trends.

Dispersion normalisation proved to be a suitable method for long-term trend assessment and for quantifying the impact of regulatory measures on air quality. Its key advantages include methodological simplicity and the availability of the input data required for the calculation of the ventilation coefficient (e.g., from ERA5).

1 Introduction

Heavy metal (HM) pollution remains a significant environmental issue due to its persistence in the environment and its harmful effects on human health and ecosystems, such as toxicity and bioaccumulation in the human body (EEA, 2013; Mitra et al., 2022; Suvarapu and Baek, 2017). Once released into the atmosphere, HMs can be absorbed onto aerosol particles, which can then be inhaled, leading to severe health issues. Additionally, these HM-polluted particles can be deposited into soil and water, thereby contaminating the broader environment. The emission of HMs into the atmosphere is associated with anthropogenic operations, including industry, transportation, and mining activities (Ma et al., 2024)

Despite the reductions in emissions and ambient levels since the 1990s (EEA, 2024; EEA, 2025), HMs still require strict regulation as they do not degrade in nature (e.g. Ahmad et al., 2021; Briffa et al., 2020; Mitra et al., 2022). This demand is demonstrated by regulations such as the Convention on Long-range Transboundary Air Pollution (LRTAP) - Protocol on Heavy Metals, Directive 2004/107/EC, and Directive 2008/50/EC. The relevance of this issue is further underscored by the

https://doi.org/10.5194/ar-2026-15
Preprint. Discussion started: 13 April 2026

release of EU Regulation 2023/915, on maximum levels of food contamination by selected elements, including heavy metals, and Directive (EU) 2024/2881, on ambient air quality and cleaner air for Europe. In the Czech Republic, national law integrates these EU regulations and directives concerning HM emission and immission limits through Act no. 201/2012 Sb. The immission limits for selected heavy metals, such as Arsenic (6.0 ng m^{-3}), Cadmium (5.0 ng m^{-3}), Lead (500 ng m^{-3}) and Nickel (20 ng m^{-3}), have been established in the Czech Republic.

This study investigates the evolution in HM concentrations with immission limits in the Czech Republic from 2010 to 2021 (the period after a substantial lowering of HM concentrations in ambient air) across various environments, focusing on the effects of current regulations. These limits are not being exceeded long-term in most of the territory of the Czech Republic.

Central Europe is among the regions with the highest concentrations and deposition of HMs in Europe (Travnikov et al., 2020). However, air quality is significantly improving in this region (Aas et al., 2024), so we focused on these three sub-objectives in our study:

The application of dispersion normalization was used for the first time to remove the influence of meteorological changes in describing HM concentrations and trends at air quality stations.

The three main objectives were to investigate:

1. Evaluate long-term trends of HMs at different monitoring station types in the Czech Republic.
2. Investigate the suitability of the station's selection and establish a representative group. A critical research question addresses whether a single monitoring station can serve as a representative sample for the entire network or whether multiple stations are necessary to ensure data reliability. The study aims to identify potential methodological challenges and limitations associated with the selection and grouping of monitoring stations for emission assessment purposes.
3. Examine the influence of meteorological variables on measured immission concentration in relation to evaluating the manifestation of the regulation of emission amount. The study evaluates whether normalisation techniques constitute appropriate methodological tool for isolating emission signals from meteorological influence. Specifically, the study is focused on dispersion normalisation using the ventilation index. The goal of this objective is to explore the potential masking of the changes in emission by meteorological effects.

2 Sources of HMs and Emission structure in the Czech Republic

HMs are released into the atmosphere by natural and anthropogenic processes, as well as many other pollutants. The typical natural sources for studied HMs are volcanic eruption, soil erosion or soil dust and wildfires (EEA, 2013; Tchounwou et al., 2012). The primary anthropogenic sources of arsenic (As) are metal smelters and fuel combustion (EEA, 2013), manufacturing insecticides, herbicides, and similar inhibitors (Tchounwou et al., 2012). Cadmium (Cd) input into the atmosphere from anthropogenic sources is via the emission of production of non-ferrous metals, stationary fossil fuel combustion, waste incineration, etc. Anthropogenic activities that produce lead (Pb) emissions are traffic, fossil fuel combustion, waste incineration, production of non-ferrous metals, etc. Nickel (Ni) released into the atmosphere by anthropogenic sources is

https://doi.org/10.5194/ar-2026-15
Preprint. Discussion started: 13 April 2026

mainly emitted by the combustion of oil (from heating, shipping, power generation), mining, waste incineration, etc. (EEA, 2013).

The emissions in the Czech Republic changed both in terms of the amount and structure of sources between 1990 and 2021. The most dramatic evolution was recorded by the total amount of As and Pb emissions. As emissions dropped to 1.8% of the 1990 value, i.e. by 98.2%. Pb emissions decreased to 4.6%, i.e. by 95.4%. In contrast, the Cd emission amount declined only to 24% of the 1990 value, i.e. by 76% (Table 1). The diverse structure of sources between 1990 and 2021 is also visible. Whereas one of the main source sectors for almost all studied HMs was Iron and steel production in 1990, the situation was different in 2021, where the common emission source was Public electricity and heat production. The limitation of using Pb as a component of fuels is pronounced by the lowering of contribution sector Road transport: Passenger car (Fig. 1). For easier interpretation, only the first three emission sources are listed. Detailed information is accessible, e.g. CIEP (2024), CHMI 2026. The described changes prove that the restriction under CLRTAP and EU directives (mentioned in the introduction) helped lower HM concentrations and limited some sources.

Table 1: Overview of emmision total amount in 1990 and 2021 in the Czech Republic. The structure of emmision developed based on technological development and the laws regulation. Source: CEIP (2026).

Year	1990	2021	Reduction
Component	Emmision Total [t]		%*
As	69.5	1.3	98.2
Cd	5.3	1.3	75.9
Ni	55.0	4.3	92.1
Pb	316.6	14.7	95.4

* Reduction compare to 100% in 1990.

https://doi.org/10.5194/ar-2026-15
Preprint. Discussion started: 13 April 2026

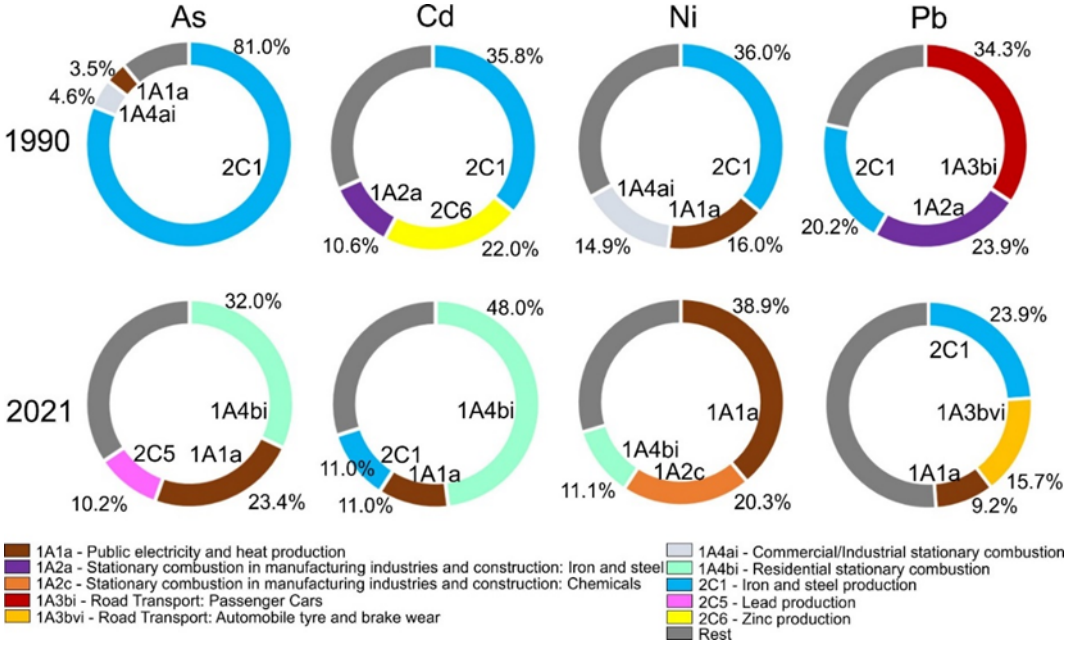

Figure 1: Structure of selected HM emmision sources according to NFR sectors in 1990 and 2021. Only first three sectors are visualised, the other sources in category rest. Source: CEIP (2026).

A similar reduction in HM emissions observed in the Czech Republic was recorded in the European context (Fig. S1). Beyond domestic emission sources, transboundary transport should be considered as a significant contributor to elevated HM concentrations. For instance, according to Travnikov et al. (2020), transboundary transport accounts for 7–99% of cadmium (Cd) deposition from non-national sources in EMEP member countries.

3 Atmospheric boundary layer and Ventilation coefficient

The meteorological conditions affect measured pollutant concentrations. Some of the meteorological parameters are spatially variable. Their involvement in the calculation of influence on pollution concentration is too complicated and ensure using complex model (Gilliam et al., 2006; Williams, 2013; Zhang, 2019). To simplify calculations of the effect of meteorological conditions on pollutant concentrations, the ventilation coefficient (VC) parameter can be used. VC_i is defined as the product of atmospheric mixing layer height (MLH_i) and wind speed (u_i) at a particular height for the selected time interval (i) (e.g. Chen et al., 2022; Ferguson, 2001), as shown in Equation (1):

$$VC_i = MLH_i \times u_i , \quad (1)$$

The relation between MLH and wind speed and air pollution is regularly studied (e.g. Ferguson, 2001; Holzworth, 1967; Iyer and Raj, n.d.; Soleimanpour et al., 2023; Venegas and Mazzeo, 1999). An example of VC calculation can be found in Ashrafi et al., 2009; Wu et al., 2023. The character of MLH is an important factor enabling the dilution of atmospheric pollution. MLH

https://doi.org/10.5194/ar-2026-15
Preprint. Discussion started: 13 April 2026

is a sublayer of the atmospheric boundary layer (ABL) that reaches heights from the ground to hundreds of meters and units of kilometres. The dominant turbulent motion in this layer is driven by mechanical and thermal convection. Mechanical effect is the result of wind shear, thermal convection is caused by the interaction of Earth's ground with incoming solar radiation and subsequent transfer of heat to a relatively cooler atmosphere (Berg et al., 2013; Stull, 2003, 2016). The diurnal height variation of MLH and ABL is the result of the character of meteorological factors, such as temperature, moisture, solar radiation, wind, turbulence, etc. (Stull, 2016).

The VC and MLH parameters capture the evolution of key meteorological factors and can be used for dispersion normalisation. Accounting for meteorological conditions allows for more reliable evaluation and comparison of concentration data.

4 Methods

4.1 Selection of stations

HMs are regularly monitored within the National Air Quality Monitoring Network of the Czech Hydrometeorological Institute (CHMI). This monitoring network comprises over 30 manual stations and about 100 automatic air quality stations. However, for this study, only results from manual stations were suitable. Further station selection was necessary to evaluate results only from the measurement with a complete data series of all selected parameters from 2010 to 2021. The data series had to fulfil criteria set in Directive 2008/50/EC, Annex I and Directive 2004/107/EC, Annex IV for the presentation and validity of air pollution characteristics. Which is a minimum of 90% data coverage in an individual time period (CHMI, 2023). Under these

https://doi.org/10.5194/ar-2026-15
Preprint. Discussion started: 13 April 2026

115 rules, 16 stations across the Czech Republic were selected for this study (Fig. 2). These stations are located in different geographical areas.

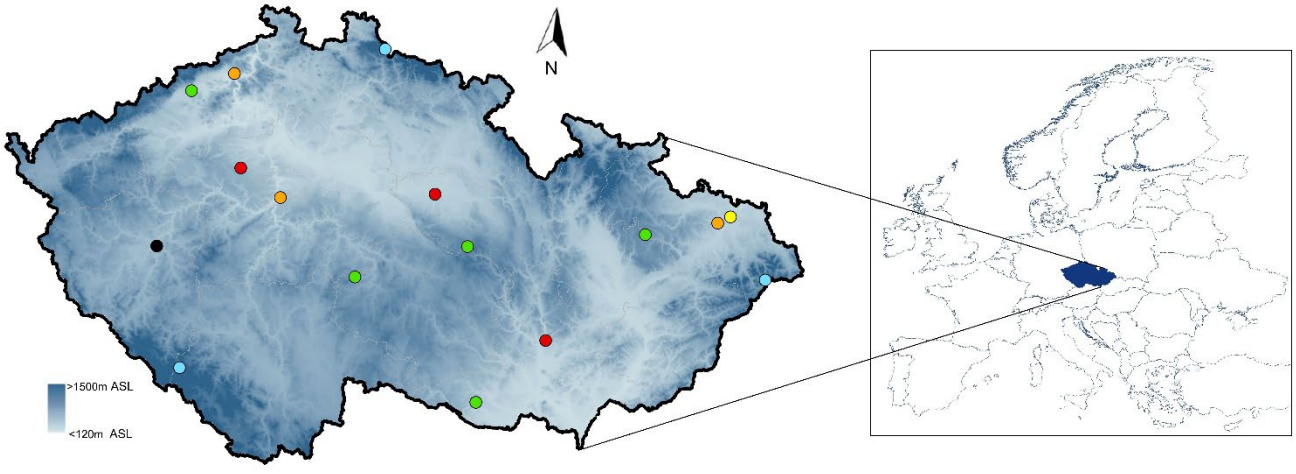

120 **Figure 2: Spatial distribution of selected stations measured HM in period 2010–2021, Czech Republic, Europe. Colours representing particular station type. Background Rural Mountain stations – BRM are coloured lightblue, Background Rural Lowland stations – BRL green, Background Urban stations - BU red, Background Suburban stations - BS orange, Industrial station I – yellow and Traffic station – T black. The map data were proccessed in ArcGis programme (ESRI, 2018).**

Data were processed and evaluated in individual categories based on station type and altitude. The dataset was split into the following six categories: Background Rural Mountain stations – BRM, Background Rural Lowland stations – BRL, 125 Background Urban stations – BU, Background Suburban stations – BS, Industrial station I, and Traffic station – T. Basic characteristics are listed in Table S1. The categorization was done according to EOI classification, which is based on Council Decision 97/101/EC (CHMI, 2023). Background rural stations were split into two subcategories based on altitudes of stations. The border between lowland and mountain was set to 800 m a.s.l.

The one criterion for data processing was to maintain consistency and comparability within the time series (the period 2010–130 2021 was chosen). Data after 2021 may exhibit minor inconsistencies, as technical issues with laboratory devices in 2022 and subsequent years resulted in temporary delays in analyses and limited gaps in the dataset.

4.2 Dispersion normalization

Data set covers 12 years of data measured under different meteorological conditions. Therefore, the right evaluation needs 135 data normalization and exclusion of meteorological conditions. The reduction of meteorological influence was calculated according to recently developed method intended for dispersion normalization of Positive Matrix Factorization (DN-PMF)

https://doi.org/10.5194/ar-2026-15
Preprint. Discussion started: 13 April 2026

analysis. This approach is widely used by research community (e.g. Alfeus et al., 2024; Chen et al., 2022; Hopke, 2021; Mbengue et al., 2023; Wu et al., 2023; Yang et al., 2022). Dispersion normalization (DN) concentration is calculated according to Equation (2):

$$C_{DN} = C_i \times \frac{VC_i}{\overline{VC}}, \quad (2)$$

Where C_{DN} is dispersion normalized concentrations, C_i means measured concentration, VC_i is value of ventilation coefficient and $\overline{VC}$ is averaged ventilation coefficient under whole studied period.

VC in this study is used from Numerical Weather Prediction model Aladin operation by CHMI. Calculation of VC for Czech condition is based on methodology listed in Ferguson (2001) and for calculation is used thickness of MLH and average wind speed in MLH (Škáchová, 2020; Škáchová and Keder, 2025).

4.3 Long-term trends

Trends in concentrations of individual components were evaluated using the Theil-Sen method (Carslaw and Ropkins, 2012; Sen, 1968; Theil, 1950), which is based on the non-parametric Mann-Kendall approach. This combination makes effective tool for analyzing nonparametric data. In this analysis, the mean monthly values of the 75th or 95th percentiles of concentrations are considered (used e.g. in Lhotka et al., 2019).

The average slope of the trend, denoted by the T parameter, is calculated as follows, Equation (3):

$$T[\% \cdot yr^{-1}] = 100 \cdot \left(\frac{C_{End}}{C_{Start}} - 1\right) / N_{years}, \quad (3)$$

where:

N_{years} is the number of years over which measurements were taken.

C_{End} and C_{Start} represent the mean concentrations at the end and start of the measurement period, respectively.

The long-term trends were evaluated for both original and normalised data; however, the main focus was on the HM_{DN} results.

4.4 Sampling and analysing methods

The evaluated data were obtained from direct sampling at the selected stations. Each station measured the concentration of selected HMs in size fraction PM_{10} with a sequential sampling device (sequential sampler SQ47/50, Sven Leckel, Germany). The measurement was scheduled in frequency 1×2 days; the air was continuously sampled for 24 hours starting at 0:00 UTC. Samples were, after exposure, analysed in accredited laboratories of CHMI (according to the ČSN EN ISO/IEC 17025 standard) by mass spectrometry with inductively coupled plasma (ICP-MS) method (CHMI, 2023).

https://doi.org/10.5194/ar-2026-15
Preprint. Discussion started: 13 April 2026

5 Results

5.1 Basic overview of HM concentrations measured at different station types

The HM concentrations varied according to station type. The lowest concentrations were observed at mountain background stations (BRM), where median values reached 0.35 ng m^{-3} for As, 0.08 ng m^{-3} for Cd, 0.21 ng m^{-3} for Ni, and 2.1 ng m^{-3} for Pb. The second category exhibiting relatively low concentrations is represented by lowland background stations (BRL), with median concentrations of 0.54 ng m^{-3} for As, 0.09 ng m^{-3} for Cd, 0.33 ng m^{-3} for Ni, and 2.57 ng m^{-3} for Pb. Background suburban (BS), background urban (BU), and traffic (T) stations demonstrated comparable concentration levels across all evaluated HMs. Notably, As concentrations were elevated at BU and T station types, while Ni concentrations at traffic station differed from those recorded at BU and BS locations. Ni at T station differed from BU and BS. The median concentrations at BS, BU, and T stations were 0.79, 0.88, and 0.96 ng m^{-3} for As; 0.13, 0.14, and 0.14 ng m^{-3} for Cd; 0.48, 0.51, and 0.64 ng m^{-3} for Ni; and 4.70, 4.61, and 4.36 ng m^{-3} for Pb, respectively. The highest concentrations were measured at industrial (I) station type. The median As concentration reached 1.72 ng m^{-3}, Cd 0.33 ng m^{-3}, Ni 1.64 ng m^{-3} and Pb 14.90 ng m^{-3} (Fig. 3). Comparison between OR and DN results is visualise in Fig. S2.

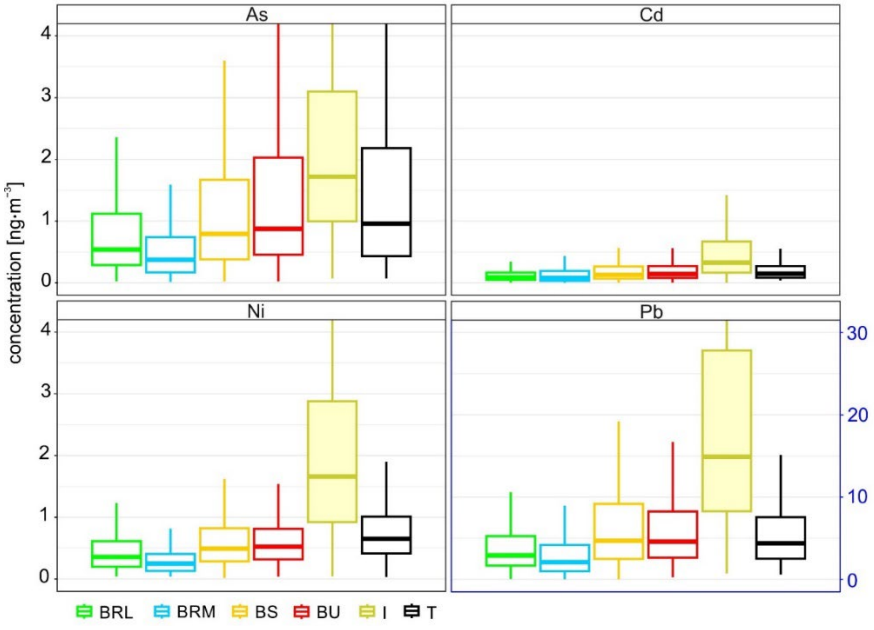

Figure 3: HM concentration overview at all station type, 2010–2021. Colours representing particular station type. Background Rural Lowland stations – BRL green, Background Rural Mountain stations – BRM are coloured lightblue, Background Suburban stations – BS orange, Background Urban stations – BU red, Industrial station I – yellow and Traffic station – T black.

https://doi.org/10.5194/ar-2026-15
Preprint. Discussion started: 13 April 2026

AEROSOL Research Discussions

5.2 Integration of stations into groups

The stations were selected based on the availability of time-series data and grouped by type (according to EOI classification) and geographical location. The group's representativeness was necessary to test its eligibility and confirm the relevance of the presented results. The data used for this verification was HM_{DN} to exclude the meteorological variability at individual stations.

5.2.1 Correlation between individual stations and particular HM_{DN}

In order to compare the results from individual stations, Spearman's correlation coefficient (R_s) values were calculated for HM_{DN} concentrations (Table S2–5). The correlation results were evaluated primarily for individual HM_{DN} between station pairs. Following (Mukaka, 2012) and (Schober and Schwarte, 2018), $R_s = 0.70$ was chosen as the threshold for strong correlation. For As_{DN}, nine pairs of stations showed strong correlations, with the strongest observed for LOM ($R_s > 0.7$ in 3 cases). For Cd, 22 stations pairs demonstrated strong correlations, most often observed for LIB ($R_s > 0.7$ in 6 cases) and EPA ($R_s > 0.7$ in 6 cases) and for KOS and LOM ($R_s > 0.7$ in 5 cases). No stations pairs with strong correlations were identified for Ni_{DN} (R_s 0.22–0.54). For Pb_{DN}, 19 pairs of station showed strong correlations, most frequently involving KOS ($R_s > 0.7$ in 5 cases) and KUCH, ESV, LIB, BBN, and EPA ($R_s > 0.7$ in 4 cases each). These results suggest that Cd and Pb sources were relatively uniform across the Czech Republic and, by extension, Central Europe. In contrast, Ni concentrations and sources showed the most variability among all evaluated HM_{DN} (confirming the findings presented in Sections 5.2.2 and 5.3.1). The lowest correlations ($R_s < 0.6$) were found for HM_{DN} concentrations at BRM stations. Dissimilar air masses impacting these locations on the Czech Republic's borders likely amplify differences between the stations compared to those at inland locations. Frequently, low R_s occurred at the OPR industrial station, especially for As and Pb. These differences could be due to specific sources of As and Pb emissions in the Ostrava region (steelworks, metallurgical plants, and mines).

The overall R_s result indicates that the relationship among station results is also influenced by their mutual distance (Fig. 4). High R_s values (over 0.77) were found for OPR and OPO, BBN and KUCH, and LIB and SKL stations (except Ni_{DN}). When comparing correlations between the all four studied HM_{DN} at one station (Table S6–9), the highest correlation coefficients were found for Pb–Cd pairs (R_s = 0.72–0.94, median = 0.90) and Pb–As pairs (Rs = 0.70–0.87, median = 0.76), which could be related to their similar sources (industrial production/public energy/residential heating). An exception is the correlation between Pb and Cd at JIZ (R_s = 0.62), where the glass industry influences Cd concentrations. Conversely, the lowest correlations were found for Ni–As and Ni–Pb pairs (R_s = 0.32–0.66), confirming a different trend in Ni concentrations compared to the remaining HMs.

https://doi.org/10.5194/ar-2026-15
Preprint. Discussion started: 13 April 2026

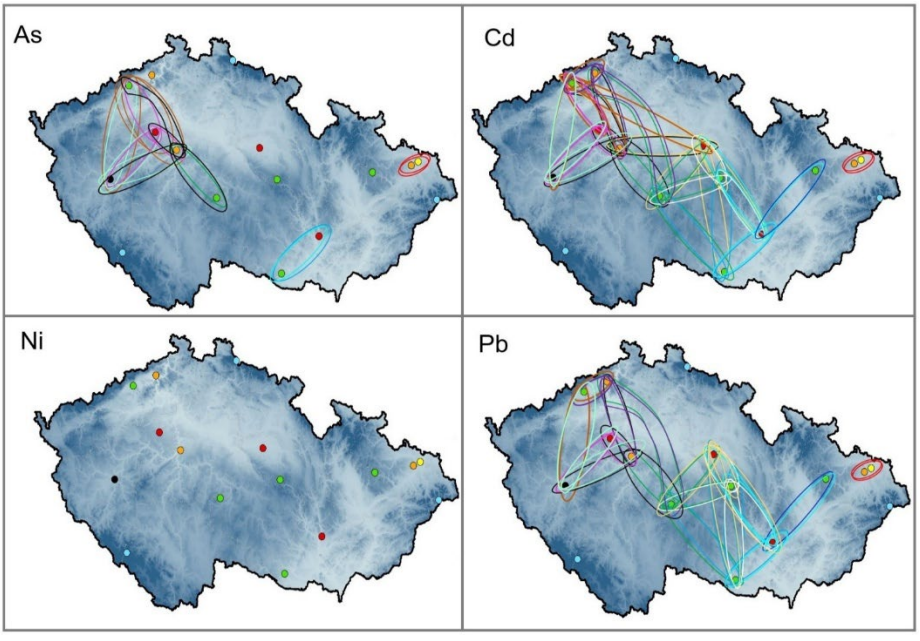

Figure 4: The spatial relationships among stations according to individual HM_{DN} R_s values > 0.7. Colours of dots representing particular station type. Background Rural Mountain stations – BRM are coloured lightblue, Background Rural Lowland stations – BRL green, Background Urban stations - BU red, Background Suburban stations - BS orange, Industrial station I – yellow and Traffic station – T black.

5.2.2 Verification by the HM_{DN} long-term trend

Each station and the particular HM were evaluated separately for the long-term trend evolution (decreasing/increasing/stable) and its statistical significance. The As_{DN} concentration trend was generally decreasing ($p < 0.001$) at all stations (Table 2). Except for three stations. The LOM and ESV station (both BRL station types) show a slight decreasing trend with no statistical significance. EPA station (BU) was characterised by a decreasing trend on significance level $p < 0.5$ (Table S10). Results from the trend calculations for Cd_{DN} and Pb_{DN} concentrations showed not only a decreasing trend at the highest significance level across groups, but also for all individual stations. The Ni_{DN} concentrations differed during the study period from those of the remaining HMs. The concentration trend analyses from individual stations are consistent with the overall trend analyses for groups. Note that BMR trend results show a significant trend $p < 0.001$; however, two stations BKR and CHU station shows descresing trend on lower significance level ($p < 0.01$). Similar situation occurred for BS stations. The overall BS trend was at significant level $p < 0.001$, however ULK station indicated decreasing trend on $p < 0.01$ and OPO showed very slight decreasing tendency with no statistically significant trend. The industrial station OPR is represented by slight increasing tendency with no statistically significant trend.

https://doi.org/10.5194/ar-2026-15
Preprint. Discussion started: 13 April 2026

The individual HM concentrations trend analyses confirmed that the data series from individual stations are suitable for group calculations and further evaluation. However, the individual behaviour of HM concentrations at a particular station should be taken into account in the data interpretation.

The statistical significance results were the same for the grouped HM_{DN} and HM datasets. However, the percentage increase/decrease and confidence interval values were higher for HM results (Table 2).

Table 2: The results of long-term trend analyses of HM concentrations for the grouped station (according to station type – EOI classification and altitude). Background Rural Lowland stations – BRL, Background Rural Mountain stations – BRM, Background Suburban stations – BS, Background Urban stations – BU, Industrial station I and Traffic station – T. The overall trend is mentioned as a percentage increase/decrease per year, and the 95 % confidence intervals in the slope are listed in [ ] %/year. Significance level: p < 0.001 = ∗ ∗ ∗.

Station type	As %/year	Cd %/year	Ni %/year	Pb %/year
BRL_{DN}	−3.76 [−4.76, −2.41] ***	−4.6 [−5.56, −3.63] ***	−3.39 [−4.29, −2.05] ***	−4.54 [−5.67, −3.65] ***
BRL	−4.73 [−6.11, −3.50] ***	−5.65 [−6.97, −4.16] ***	−3.56 [−4.64, −2.29] ***	−5.39 [−6.26, −4.25] ***
BRM_{DN}	−5.06 [−5.94, −4.19] ***	−5.93 [−6.63, −4.90] ***	−4.00 [−4.71, −2.90] ***	−4.76 [−5.48, −3.89] ***
BRM	−5.76 [−6.67, −4.96] ***	−6.82 [−7.79, −5.85] ***	−4.62 [−5.29, −3.81] ***	−5.46 [−6.10, −4.75] ***
BS_{DN}	−4.27 [−5.74, −2.70] ***	−6.18 [−7.15, −5.32] ***	−3.07 [−3.98, −2.01] ***	−5.78 [−6.72, −4.66] ***
BS	−4.17 [−5.56, −2.30] ***	−6.24 [−7.05, −5.08] ***	−3.14 [−3.97, −2.03] ***	−5.90 [−6.95, −4.75] ***
BU_{DN}	−3.46 [−4.81, −2.12] ***	−5.44 [−6.55, −4.30] ***	−3.66 [−4.48 −2.73] ***	−5.46 [−6.33, −4.30] ***
BU	−4.61 [−5.49, −3.10] ***	−5.99 [−7.27 −4.63] ***	−4.02 [−4.83 −3.05] ***	−6.16 [−6.94, −4.92] ***
I_{DN}	−3.73 [−4.87, −2.63] ***	−5.73 [−6.60, −4.73] ***	0.74 [−1.68, 4.14]	−4.95 [−5.82, −4.01] ***
I	−4.41 [−5.66 −3.42] ***	−6.19 [−7.44, −5.26] ***	0.23 [−1.8, 3.31]	−5.85 [−6.54, −5.09] ***
T_{DN}	−4.54 [−6.31, −2.54] ***	−5.36 [−6.89, −4.08] ***	−5.02 [−5.92, −3.97] ***	−5.86 [−6.77, −5.50] ***

https://doi.org/10.5194/ar-2026-15
Preprint. Discussion started: 13 April 2026

T	−5.09 [−6.41, −3.00] ***	−6.04 [−7.16, −4.72] ***	−4.81 [−5.84, −3.78] ***	−6.52 [−7.34, −5.49] ***

5.3 HM concentrations and patterns across station types

Across all investigated HMs, a divergence between original (OR) and dispersion normalised (DN) concentration datasets was observed, indicating meteorological influence on measurement immission. The magnitude of differences varies among station types. The stable response to meteorological conditions was recorded at BRM (OR and DN difference interval was 19–51%) and BRL stations (OR and DN divergence reached 12–39%). However, the topography or microenvironmental characteristics were most evident at the T station type (OR–DN range: 8–52%), where street canyon effects and building configurations probably modify meteorological influences on pollutant dispersion and accumulation. The OR–DN convergence over the years has predominantly ranged from 7 to 52% across station types and the studied HM. The highest OR–DN convergence was observed in 2017 across the entire dataset (OR–DN range: 8–35%), indicating good dispersion conditions reflected at all HM and environmental types. Especially for Cd (BU and I) and Pb (BU and T).

All station types exhibit statistically significant declines in As, Cd, Ni and Pb ($p < 0.001$), providing clear evidence of the effectiveness of emission-reduction policies. The consistency of these trends across rural, suburban, urban, industrial, and traffic environments highlights the regional-scale impact of legislative measures rather than isolated local improvements. The specific behaviour was recorded in Ni; the constant OR–DN divergence occurred at all station types. No trend was observed for the I station, which is an unusual pattern in the datasets studied.

5.3.1 Concentrations of As, Cd, Pb, and Ni at different station types

Arsenic shows statistically significant declines across all station types ($p < 0.001$), with annual reduction rates ranging from 3.45% (BU) to 5.93% (BRM). This universal pattern confirms the effectiveness of legislative measures targeting As emissions. The highest As_{DN} concentrations were recorded at I station (0.83–1.92 ng m^{-3}), as expected, because industry is the primary source of As. As_{OR}–As_{DN} range: 7–47% probably reflected not only episodic emission events but also changes in meteorological influences. The short-term increase in emission enrichment during 2011–2013 was partially masked by meteorological conditions in the As_{OR} data at the T and I stations. In those cases, the added value of the DN method is visible. The cleanest monitoring environment was BRM - As_{DN}, with values ranging from 0.13 to 0.32 ng m^{-3} (Fig. 5).

https://doi.org/10.5194/ar-2026-15
Preprint. Discussion started: 13 April 2026

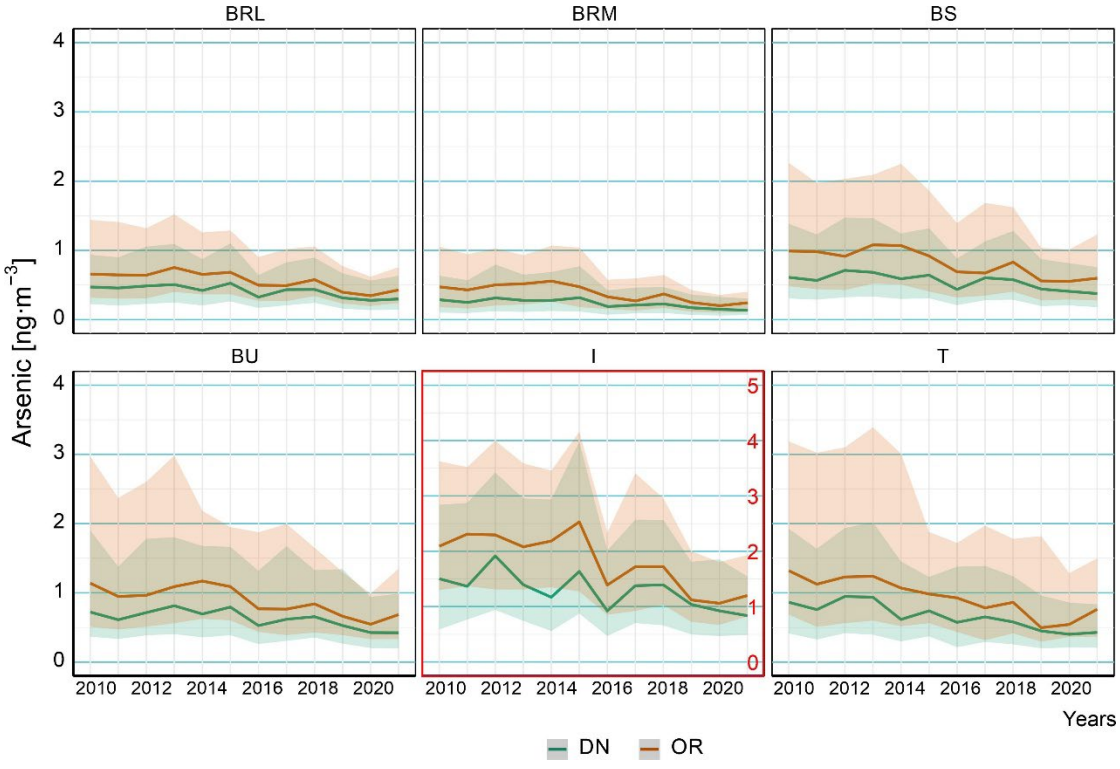

Figure 5: Arsenic concentration at Background Rural Lowland stations – BRL, Background Rural Mountain stations – BRM, Background Suburban stations – BS, Background Urban stations – BU, Industrial station – I and Traffic station – T, 2010–2021. The green line shows the median concentration of dispersion normalised data (DN), and the orange line is the median concentration of the original data series (OR). The coloured area visualises the interquartile range (25th–75th percentile).

Cadmium exhibits statistically significant declining trends across all station types ($p < 0.001$), with annual reduction rates ranging from 4.77% (BRL) to 6.15% (BS). The highest reduction rate at BS is probably connected with emission control measures – reflecting a combination of traffic emission reductions and decreased industrial activity in peri-urban zones. The meteorological influence pattern is evident during 2010–2014, when Cd_{OR}–Cd_{DN} ranged from 20% to 52% across all environments. However, from 2015, better dispersion conditions were observed (Cd_{OR}–Cd_{DN}: 8%–46%) at several stations (BRL, BRM, BS, BU, I), particularly in 2017. Cd_{OR}–Cd_{DN} convergence was probably a result not only of the stabilisation of meteorological conditions but also of emission sources steadying (Fig. 6).

https://doi.org/10.5194/ar-2026-15
Preprint. Discussion started: 13 April 2026

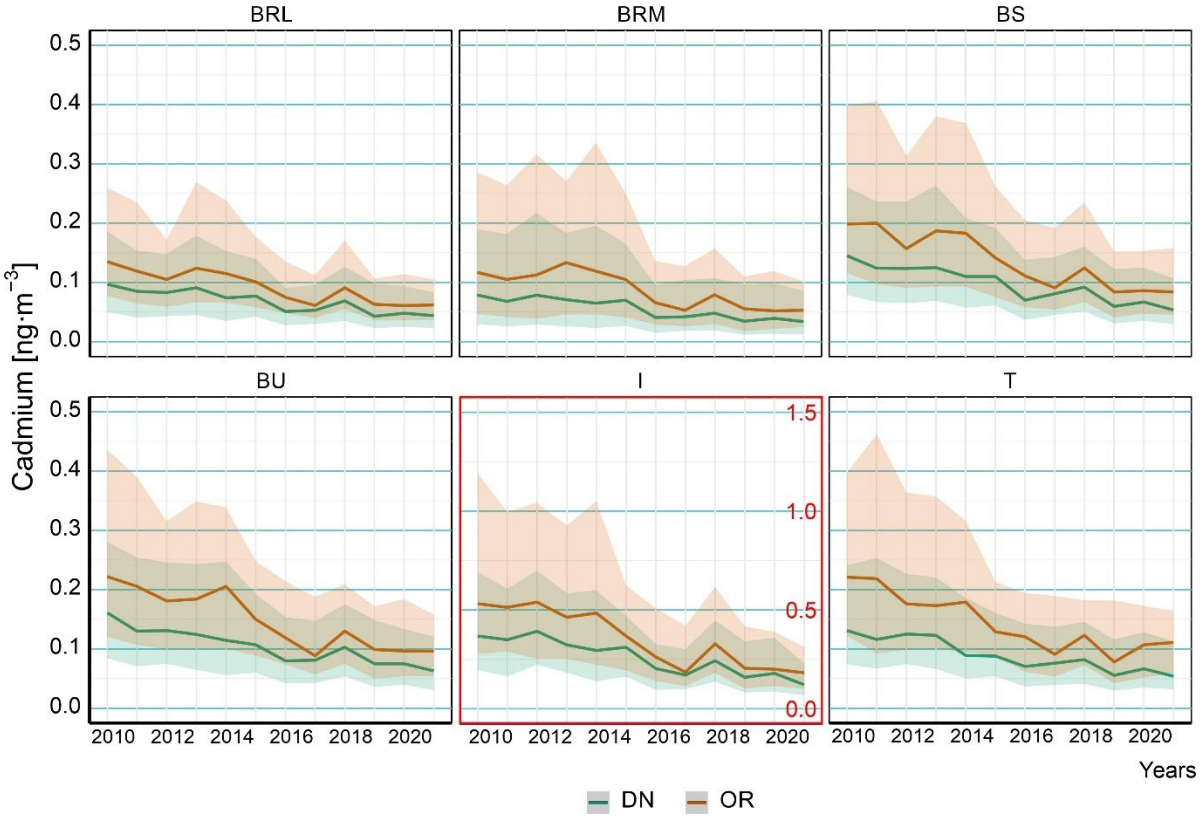

Figure: 6 Cadmium concentration at Background Rural Lowland stations – BRL, Background Rural Mountain stations – BRM, Background Suburban stations – BS, Background Urban stations – BU, Industrial station – I and Traffic station – T, 2010–2021. The green line shows the median concentration of dispersion normalising data (DN), and the orange line is the median concentration of the original data series (OR). The coloured area visualises the interquartile range (25th–75th percentile).

The evolution of Ni concentration was in line with As, Cd, and Pb. Statistically significant declining trends were observed at all station types except I station. Annual reduction rates ranging from 3.07% (BS) to 5.02% (T) show no significant trends. The industrial sources probably suppress the regulatory measures more effectively than other HMs. Ni emissions were governed by sources with an operation regime less affected by seasonality (industrial processes, traffic – tyres and brakes abrasion). The consistently high OR–DN divergence (20–50%) indicates that nickel atmospheric behaviour is sensitive to meteorological conditions, expressed in all environments (Fig. 7).

https://doi.org/10.5194/ar-2026-15
Preprint. Discussion started: 13 April 2026

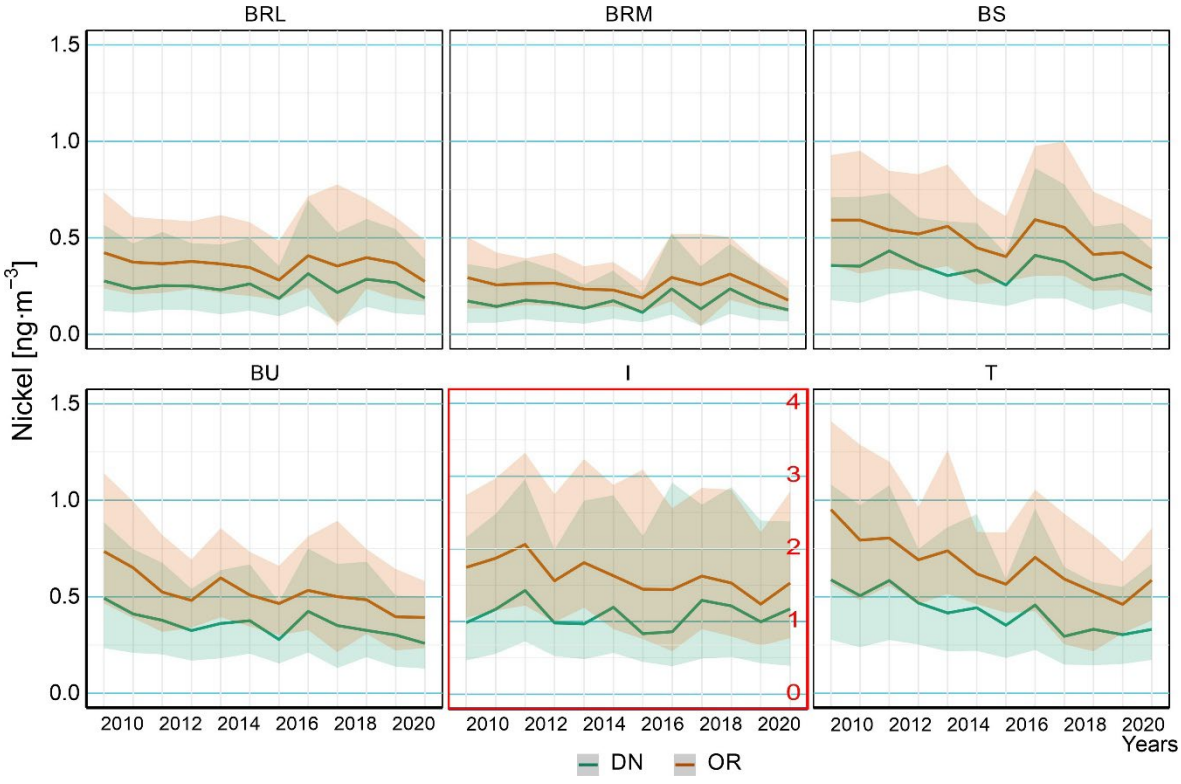

Figure 7: Nickel concentration at Background Rural Lowland stations – BRL, Background Rural Mountain stations – BRM, Background Suburban stations – BS, Background Urban stations – BU, Industrial station – I and Traffic station – T, 2010–2021. The green line shows the median concentration of dispersion normalising data (DN), and the orange line is the median concentration of the original data series (OR). The coloured area visualises the interquartile range (25th–75 percentile).

Lead demonstrates the most pronounced concentration reductions across the monitoring network, with statistically significant declines at all station types ($p < 0.001$) and annual reduction rates ranging from 4.59% (BRL) to 5.87% (T). The concentration level at the I station type (6.07–16.69 ng m^{-3}) was an order of magnitude higher than at BRM locations, which recorded the lowest concentrations (0.89–2.17 ng m^{-3}). This steep decline in Pb_{DN} likely reflects the effectiveness of lead phase-out policies in gasoline and industrial processes. The episodic peaks at I stations (2012, 2015, 2018) suggest that, despite overall declining trends, certain industrial processes continue to generate periodic increases in emissions. The exceptional meteorological sensitivity at T stations (8–50% OR–DN divergence) combined with the highest reduction rate (5.87%) demonstrates that while traffic-related Pb emissions have declined most rapidly, street canyon effects continue to create complex relationships between emissions and observed concentrations. The second-highest reduction rate of Pb_{DN} values was detected at BS station types (5.78%) (Fig. 8).

https://doi.org/10.5194/ar-2026-15
Preprint. Discussion started: 13 April 2026

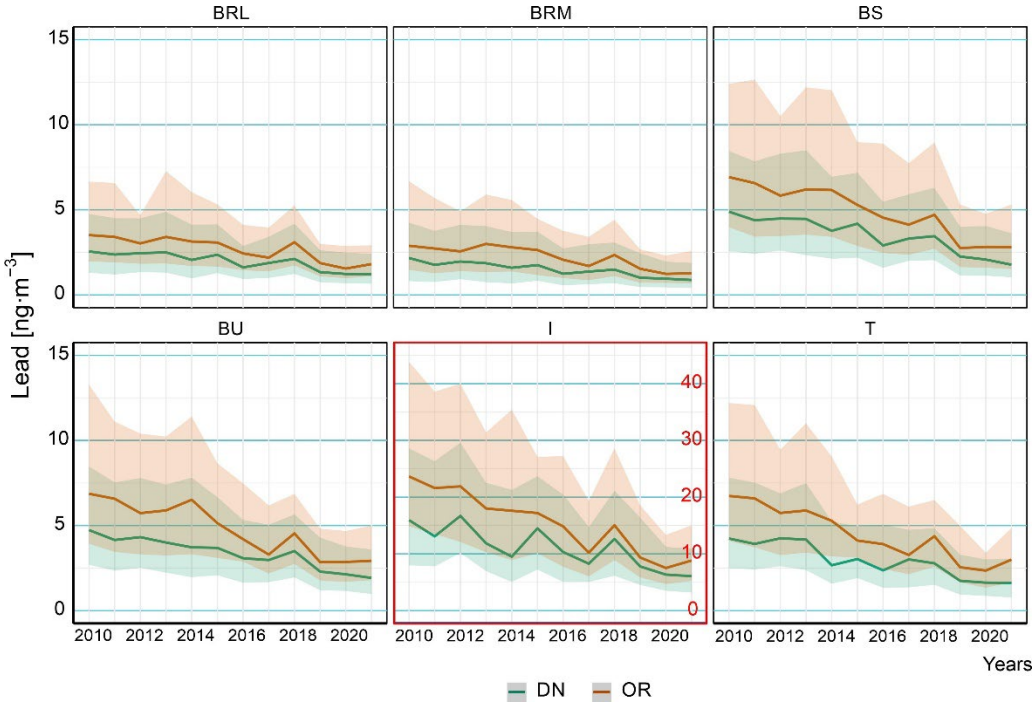

Figure 8: Lead concentration at Background Rural Lowland stations – BRL, Background Rural Mountain stations – BRM, Background Suburban stations – BS, Background Urban stations – BU, Industrial station – I and Traffic station – T, 2010–2021. The green line shows the median concentration of dispersion normalising data (DN), and the orange line is the median concentration of the original data series (OR). The coloured area visualises the interquartile range (25th–75th percentile).

The dispersion conditions at the individual station are visualised in Fig. S3 according to the method CHMI (2026) and Škáchová and Keder (2025).

5.3.2 Patterns across station types: BRL, BRM, BS, BU, I, T

BRL stations show consistent patterns for all HMs, characterised by a relatively narrow interquartile span, minimal temporal variability, and the lowest OR-DN divergence. This pattern was manifested by As_{DN} (0.28–0.51 ng m^{-3}, 12–36% divergence), Cd_{DN} (0.04–0.09 ng m^{-3}, 13–35% divergence), Ni_{DN} (0.13–0.27 ng m^{-3}, 26–39% divergence), and Pb_{DN} (1.37–2.88 ng m^{-3}, 13–36% divergence). Stable emission sources and minimal local anthropogenic influence could characterise the BRL environment. HM_{DN} concentrations (As, Cd, Ni and Pb) demonstrate statistically significant declining trends (3.75%, 4.77%, 3.39 % and 4.59% annually, respectively; $p < 0.001$).

BRM stations recorded the lowest concentrations of HM (As_{DN} N: 0.13–0.32 ng m^{-3}, Cd_{DN}: 0.03–0.08 ng m^{-3}, Ni_{DN}: 0.06–0.17 ng m^{-3} and Pb_{DN}: 0.89–2.17 ng m^{-3}), confirming the least anthropogenically impacted monitoring locations. BRM stations are represented by permanent OR-DN divergence (As: 20–50%, Cd: 21–47%, Ni: 31–49%, Pb: 19–43%; Table S11), indicating pronounced meteorological sensitivity. Probably, long-range atmospheric transport and meteorological dispersion were the

https://doi.org/10.5194/ar-2026-15
Preprint. Discussion started: 13 April 2026

dominant factors controlling the HM concentrations in this clean environment. The BRM stations demonstrate the highest annual reduction rates for Cd_{DN} (5.93%, $p < 0.001$), subsequently reductions for As_{DN} (5.06%, $p < 0.001$) and Pb_{DN} (4.75%, $p < 0.001$) and Ni (4.00%, $p < 0.001$).

BS stations recorded the mean HM_{DN} concentration within the studied data series (As: 0.37–0.71 ng m^{-3}, Cd: 0.05–0.14 ng m^{-3}, Ni: 0.21–0.43 ng m^{-3}, Pb: 1.77–4.89 ng m^{-3}), reflecting the transitional nature between rural and urban environments. The highest annual reduction rates for Cd_{DN} (6.15%, $p < 0.001$) and Pb_{DN} (5.78%, $p < 0.001$) is probably a result of emission control measures. The OR-DN divergence at BS stations (As: 11–44%, Cd: 11–40%, Pb: 18–38%; Table S11) could be influenced by the local and regionally transported and changes in meteorological conditions (except Ni: 20–46%).

BU stations were represented by concentration levels exceeding concentration at BRL and BS stations (As_{DN}: 0.42–0.81, Cd_{DN}: 0.06–0.16 ng m^{-3}, Ni_{DN}: 0.21–0.49 ng m^{-3}, Pb_{DN}: 1.92–4.74 ng m^{-3}) with a broader interquartile span. OR-DN divergence within particular HM (As: 20–41%, Cd: 8–44%, Ni: 20–40%, Pb: 9–42%; Table S11) could be caused by fluctuating emission sources and dynamics of meteorological conditions in the urban environment. The lowest annual reduction rates among all station types were observed for As_{DN} (3.46%, $p < 0.001$); the remaining HMs showed decreases of Cd: 5.37%, Pb: 5.72%, Ni: 3.66% ($p < 0.001$). Despite the gradual decline, the influence of local sources or unfavourable meteorological conditions occurred episodically in the BU environment (e.g. 2014).

Industrial stations consistently recorded the highest HM concentrations (As_{DN}: 0.83–1.91 ng m^{-3}, Cd_{DN}: 0.12–0.36 ng m^{-3}, Ni_{DN}: 0.83–1.42 ng m^{-3}, Pb_{DN}: 6.07–16.69 ng m^{-3}), confirming their proximity to major emission sources. The episodic emission events and the response to dispersion conditions are reflected in the OR-DN divergence (As: 7–47%, Cd: 8–39%, Ni: 20–47%, Pb: 15–46%; Table S11). The periodic influence of local emission sources was recorded, e.g., for Pb in 2012, 2015, and 2018. Despite the highest HM_{DN} concentrations, medium annual reduction rates were observed (As: 3.73%, Cd: 5.73%, Pb: 4.94%; all $p < 0.001$). Ni_{DN} shows a slight, non-significant increase (0.74%), suggesting that although emission controls have been partially effective, the continued influence of industrial sources may be present in this location. Additionally, Ni_{DN} annual concentrations exceeded 1.00 ng m^{-3} in half of the study period, indicating the presence of Ni emission sources.

At T station, concentration ranges for As_{DN}: 0.40–0.95 ng m^{-3}, Cd_{DN}: 0.06–0.13 ng m^{-3}, Ni_{DN}: 0.30–0.59 ng m^{-3}, Pb_{DN}: 1.62–4.26 ng m^{-3}. The high annual reduction rates were registered for all HMs - As_{DN} (4.50%, $p < 0.001$), Cd_{DN} (5.20%, $p < 0.001$), Ni_{DN} (5.02%, $p < 0.001$) and Pb_{DN} (5.87%, $p < 0.001$). The declining trend is a result of a reduction in traffic-related emissions, possibly indicating the effectiveness of policies targeting vehicular emissions, including fuel quality improvements and fleet modernisation. OR-DN divergence range (As: 9–44%, Cd: 20–52%, Pb: 8–50%, Ni: 27–50%; Table S11) showed not only the influence of emission sources (probably ground-level emission) but also the dispersion conditions connected with street canyon effects.

https://doi.org/10.5194/ar-2026-15
Preprint. Discussion started: 13 April 2026

6 Discussion

The present study demonstrates the positive impact of international and European legislative measures on HM concentrations in ambient air in the Czech Republic, while also highlighting the continuing influence of industrial sources. The observed total annual declines in HM concentrations (1.7–8.1% per year) are substantially higher than the decline in total PM_{10} concentrations across European background stations (1.8% per year) reported by Aas et al. (2024). This contrast supports the assumption that regulatory measures specifically targeting HM emissions have been more effective than general particulate matter mitigation strategies.

Comparable long-term trends were reported by Kyllönen et al. (2020), who evaluated HM concentrations at a subarctic background station in Finland. However, their study identified lower levels of statistical significance for As (no significant trend), Cd and Ni ($p < 0.05$), and Pb ($p < 0.001$) during the overlapping period. In contrast, our results show statistically significant decreasing trends ($p < 0.001$) for most station types and metals, indicating that emission-reduction measures probably had a stronger impact in Central Europe, where industrial density and historical emission burdens were considerably higher.

A notable feature in the time series is the elevated HM concentrations observed in 2018. This increase coincided with the exceptionally dry and warm spring–summer period that affected large parts of western, northern, and central Europe (Bastos et al., 2020). The prolonged drought reduced wet deposition and enhanced atmospheric stability, leading to the accumulation of pollutants, including heavy metals, in the atmosphere. Similar meteorologically driven increases in pollutant concentrations and deposition have been documented within the EMEP network (Travnikov et al., 2020). This finding supports the need for dispersion normalisation approaches to disentangle emission trends from meteorological variability.

The year 2018 serves as an example of how meteorological conditions can mask or amplify true emission signals in measured immission data. In the present study, the divergence between original (OR) and dispersion-normalised (DN) concentrations reached up to 52% across station types and individual metals, demonstrating a substantial impact of atmospheric dispersion conditions on measured concentrations, particularly during years with unfavourable dispersion conditions, notably in the cold season of 2010–2013. Another such example is the increase in As and Cd concentrations at a traffic station during 2020 and 2021, which could be incorrectly attributed to the impact of coronavirus pandemic-related restrictions. However, our results suggest that these increases were more likely attributable to adverse meteorological dispersion conditions rather than changes in emission levels. Without dispersion normalisation, such meteorologically induced anomalies could be incorrectly interpreted as actual changes in emission levels. The ventilation coefficient (VC), which combines mixing layer height (MLH) and wind speed, proved to be an effective parameter for capturing the dominant meteorological factors influencing pollutant dispersion. By applying DN, the underlying emission-driven trends become more identifiable, providing a more robust basis for assessing the effectiveness of legislative measures. This methodological approach is particularly valuable in datasets spanning multiple years, where interannual meteorological variability, as documented by Travnikov et al. (2020), who reported concentration changes of up to ±50% attributable solely to meteorological variability, could otherwise obscure long-term trends. The only

https://doi.org/10.5194/ar-2026-15
Preprint. Discussion started: 13 April 2026

location of all observed stations and HMs that exceeded the air pollution limit (specifically for As) was the SKL station (urban background station type). The annual air pollution limit for As (6.0 ng·m^{-3}) was exceeded here in 2010, 2012, and 2013. The elevated As concentrations at this station are consistent with the influence of residential coal combustion, a well-documented source of As in urban environments, particularly during the heating season.

Urban stations HM concentrations in the Czech Republic can be compared with mean values reported for two urban background stations in Germany during 2008–2010 (Dimitriou and Kassomenos, 2017). While As concentrations were higher at Czech urban stations, Cd and Pb concentrations at German urban stations were comparable to those measured across Czech urban, industrial, and traffic sites. In contrast, Ni concentrations at German urban sites exceeded those observed at Czech industrial locations. The German study identified traffic as the dominant source of As, Cd, and Pb, whereas fuel oil combustion for residential heating was the primary source of Ni. These different source characteristics (traffic for As, Cd, and Pb vs. oil combustion for Ni) are consistent with the spatial patterns observed in our dataset, particularly the distinct behaviour of Ni at individual monitoring sites and the different trends of Ni at the industrial station.

According to the European Environment Agency EEA (2026), a continued overall decline in HM emissions has been observed across the EU, confirming the long-term effectiveness of legislative frameworks such as the CLRTAP Heavy Metals Protocol and EU air quality directives. Nevertheless, Germany and Poland – two countries bordering the Czech Republic – remain among the largest HM emitters in the EU. Notably, Poland showed one of the smallest reductions in Cd (−2.7%) and Pb (−17.6%) emissions between 2005 and 2023. Given the documented importance of transboundary transport in Central Europe (Travnikov et al., 2020), it is reasonable to assume that long-range transport contributes to the measured concentrations in the Czech Republic, particularly at background and mountain sites. Additionally, Slovakia and Hungary have been reported among countries with relatively high Pb and Cd concentrations within the EMEP region, further supporting the regional dimension of HM pollution.

Our findings of declining Pb and Cd concentrations across the Czech Republic are consistent with Hůnová et al. (2023), who examined depositional fluxes of these substances and documented a decline in Pb and Cd deposition from 2012 to 2019.

The Absence of a statistically significant trend in Ni concentrations at the industrial station is a notable exception within the dataset. This pattern may reflect the specific character of Ni emission sources in the Ostrava region, where metallurgical and processes operate independently of seasonal cycles, unlike the combustion-related sources that drive trends in other heavy metals (Font et al., 2022).

7 Conclusion

The long-term trend of HMs at different station types in the Czech Republic was evaluated with findings of a decreasing trend at the highest statistical significance level ($p < 0.001$) during the period 2010–2021. The results confirm the positive impact of restriction measures implemented after 2008; the representativeness of the results could be generalised to Central Europe, as the Czech Republic is located in the middle of Central Europe (see point 1 in the set objectives in the Introduction).

https://doi.org/10.5194/ar-2026-15
Preprint. Discussion started: 13 April 2026

The 16 stations with 12-year-long daily measurement data series were studied, and the groups were evaluated according to their classification and spatial locations. The representativeness of the group was confirmed by the statistical significance of HM concentrations at individual stations ($p < 0.001$). The 9% of cases (6 results from 64) did not confirm the decreasing trend observed at the rest of the stations, which was probably due to a specific pollution source at the location. The correlation analyses proved the spatial connection between the station, especially for Cd and Pb. The low correlation R_s (0.22–0.52) was found for Ni across all stations. Three factors demonstrated specifications of mountain locations: 1. the lowest HM concentrations, 2. the result of R_s under 0.7 among all the HM_{DN} and particular stations, 3. a constant difference of OR-DN values that fluctuates between 19 to 51%. This indicates a non-negligible influence of the dispersion conditions on HM concentrations.

Generally, it was confirmed that grouping stations by classification yields representative results for station and environmental types. However, the specificity of the pollution sources must be taken into account, so more than one station is recommended for calculating the representative group (see point 2 in the set objectives in the Introduction).

The dispersion-normalised data evolution clearly demonstrated the effects of the regulation measures. The specific meteorological conditions that characterise the dispersion from the mountains to the street canyon were observed. The OR-DN ratio confirms the potential of meteorological conditions to mask the real emission level. Our results confirm that within the law restriction evaluation, dispersion normalisation is a suitable method, providing clearer results. Although in this study, the ventilation coefficient was obtained from the Aladin model, which is not available to the broad user community, the variables used to calculate the ventilation coefficient are accessible via sources such as the Hysplit model (e.g. Rolph et al., 2017; Stein et al., 2015) or ERA5 (Copernicus Climate Change Service, 2023). The user community can apply the dispersion normalisation method without significant limitations.

Supplement link

The supplementary material is published alongside this article.

Team list

Adéla Holubová Šmejkalová - Air Quality Division, Czech Hydrometeorological Institute, Prague, 143 06, Czech Republic,
Radek Lhotka - Air Quality Division, Czech Hydrometeorological Institute, Prague, 143 06, Czech Republic,
Hana Škáchová - Air Quality Division, Czech Hydrometeorological Institute, Prague, 143 06, Czech Republic,
Jan Pacner - Air Quality Division, Czech Hydrometeorological Institute, Prague, 143 06, Czech Republic,

https://doi.org/10.5194/ar-2026-15
Preprint. Discussion started: 13 April 2026

Author contributions

AHS – Conceptualization, Methodology, Formal analysis, Supervision, Visualization, Writing (original draft preparation, review and editing); RL – Formal analysis, Resources, Writing (original draft preparation, review and editing); HŠ – Data curation, Formal analysis, Writing (review and editing); JP – Data curation, Formal analysis, Visualization, Writing (review and editing).

Competing interests

The authors declare that they have no conflict of interest.

Data availability

The data used in this article were collected and processed with support from projects (ARAMIS and ACTRIS-CZ) and the Czech Hydrometeorological Institute. Therefore, data sharing is subject to specific conditions. The data are available from the corresponding author upon reasonable request.

Acknowledgements

The authors would like to thank Dr P. Vondráková Pokorná for her expert consultation and our former colleague at CHMI, Ing. Tomáš Ištok, for his collaboration on this topic.

Financial support

This work was supported by the Technology Agency of the Czech Republic under the project SS02030031 ARAMIS – Integrated System of Air Quality Research, Assessment and Control and by the Large Research Infrastructure ACTRIS project – participation of the Czech Republic (ACTRIS-CZ – LM2023030) – Ministry of Education, Youth and Sports of the Czech Republic.

https://doi.org/10.5194/ar-2026-15
Preprint. Discussion started: 13 April 2026

References

Aas, W., Fagerli, H., Alastuey, A., Cavalli, F., Degorska, A., Feigenspan, S., Brenna, H., Gliß, J., Heinesen, D., Hueglin, C., Holubová, A., Jaffrezo, J. L., Mortier, A., Murovec, M., Putaud, J. P., Rüdiger, J., Simpson, D., Solberg, S., Tsyro, S., Tørseth, K., and Yttri, K. E.: Trends in Air Pollution in Europe, 2000–2019, Aerosol Air Qual. Res., 24, https://doi.org/10.4209/aaqr.230237, 2024.

Ahmad, W., Alharthy, R. D., Zubair, M., Ahmed, M., Hameed, A., and Rafique, S.: Toxic and heavy metals contamination assessment in soil and water to evaluate human health risk, Sci. Rep., 11, https://doi.org/10.1038/s41598-021-94616-4, 2021.

Alfeus, A., Molnar, P., Boman, J., Hopke, P. K., and Wichmann, J.: PM2.5 in Cape Town, South Africa: Chemical characterization and source apportionment using dispersion-normalised positive matrix factorization, Atmos. Pollut. Res., 15, https://doi.org/10.1016/j.apr.2023.102025, 2024.

Ashrafi, K., Shafie-Pour, and Kamalan, H.: Estimating Temporal and Seasonal Variation of Ventilation Coefficients, Int. J. Environ. Res, 3, 637–644, 2009.

Berg, J., Mann, J., and Nielsen, M.: Notes for DTU course 46100: Introduction to micro meteorology for wind energy, DTU Wind Energy E-0009 (EN), 105 pp., 2013.

Briffa, J., Sinagra, E., and Blundell, R.: Heavy metal pollution in the environment and their toxicological effects on humans, https://doi.org/10.1016/j.heliyon.2020.e04691, 1 September 2020.

Carslaw, D. C. and Ropkins, K.: openair -- An R package for air quality data analysis, Environmental Modelling & Software, 27--28, 52–61, https://doi.org/10.1016/j.envsoft.2011.09.008, 2012.

CEIP: Data viewer – reported emissions data: https://www.ceip.at/data-viewer-2/overview-dataviewers/officially-reported-emissions-data, last access: 25 October 2024.

Chen, Y., Masiol, M., Squizzato, S., Chalupa, D. C., Zíková, N., Pokorná, P., Rich, D. Q., and Hopke, P. K.: Long-term trends of ultrafine and fine particle number concentrations in New York State: Apportioning between emissions and dispersion, Environmental Pollution, 310, https://doi.org/10.1016/j.envpol.2022.119797, 2022.

CHMI: Commentary on the summary annual tabular survey, Prague, 2023. https://ovzdusi.chmi.cz/tabelarniRocenky/2023_enh/pdf/kom.pdf, last access: 25 October 2024.

CHMI: Interaktivní ročenky Českého hydrometeorologického ústavu: https://info.chmi.cz/rocenka/rocenkyOvzdusi.php, last access: 31 March 2026.

CHMI: Rozptylové podmínky: https://www.chmi.cz/kvalita-ovzdusi/imise-informacni-system-hodnoceni-kvality-ovzdusi/podklady-pro-hodnoceni-ko/hodnoceni-ko-rozptylove-podminky, last access: 30 March 2026.

Copernicus Climate Change Service: ERA5 hourly data on single levels from 1940 to present: https://cds.climate.copernicus.eu/datasets/reanalysis-era5-single-levels?tab=overview, last access: 30 March 2026.

https://doi.org/10.5194/ar-2026-15
Preprint. Discussion started: 13 April 2026

Dimitriou, K. and Kassomenos, P.: Airborne heavy metals in two cities of North Rhine Westphalia – Performing inhalation cancer risk assessment in terms of atmospheric circulation, Chemosphere, 186, 78–87, https://doi.org/10.1016/j.chemosphere.2017.07.138, 2017.

EEA: Air quality in Europe - 2013 report (EEA Report No 9/2013), https://doi.org/10.2800/92843, 2013.

Heavy metal emissions to air from extractive activities from 1990-2020, indexed to 1990:

Industrial pollutant releases to air in Europe:

Heavy metal emissions in Europe:

ESRI: ArcGIS 10.6, 2018.

Ferguson, S.: Smoke dispersion prediction systems., in: Smoke Management Guide for Prescribed and Wildland Fire: 2001 Edition , 163–178, 2001.

Font, A., Tremper, A. H., Priestman, M., Kelly, F. J., Canonaco, F., Prévôt, A. S. H., and Green, D. C.: Source attribution and quantification of atmospheric nickel concentrations in an industrial area in the United Kingdom (UK), Environmental Pollution, 293, https://doi.org/10.1016/j.envpol.2021.118432, 2022.

Gilliam, R. C., Hogrefe, C., and Rao, S. T.: New methods for evaluating meteorological models used in air quality applications, Atmos. Environ., 40, 5073–5086, https://doi.org/10.1016/j.atmosenv.2006.01.023, 2006.

Holzworth, G. C.: Mixing Depths, Wind Speeds and Air Pollution Potential for Selected Locations in the United States, Journal of Applied Meteorology, 6, 1039–1044, 1967.

Hopke, P. K.: Approaches to reducing rotational ambiguity in receptor modeling of ambient particulate matter, Chemometrics and Intelligent Laboratory Systems, 210, https://doi.org/10.1016/j.chemolab.2021.104252, 2021.

Hůnová, I., Kurfürst, P., Schreiberová, M., Vlasáková, L., and Škáchová, H.: Atmospheric deposition of lead and cadmium in a central european country over the last three decades, Atmosphere (Basel)., 14, https://doi.org/10.3390/atmos14010019, 2023.

Iyer, U. S. and Raj, E.: Ventilation coefficient trends in the recent decades over four major Indian metropolitan cities, n.d.

Kyllönen, K., Vestenius, M., Anttila, P., Makkonen, U., Aurela, M., Wängberg, I., Nerentorp Mastromonaco, M., and Hakola, H.: Trends and source apportionment of atmospheric heavy metals at a subarctic site during 1996–2018, Atmos. Environ., 236, https://doi.org/10.1016/j.atmosenv.2020.117644, 2020.

Lhotka, R., Pokorná, P., and Zíková, N.: Long-term trends in PAH concentrations and sources at rural background site in Central Europe, Atmosphere (Basel)., 10, https://doi.org/10.3390/atmos10110687, 2019.

Ma, X., Sha, Z., Li, Y., Si, R., Tang, A., Fangmeier, A., and Liu, X.: Temporal-spatial characteristics and sources of heavy metals in bulk deposition across China, Science of the Total Environment, 926, https://doi.org/10.1016/j.scitotenv.2024.171903, 2024.

Mbengue, S., Vodička, P., Komínková, K., Zíková, N., Schwarz, J., Prokeš, R., Suchánková, L., Julaha, K., Ondráček, J., Holoubek, I., and Ždímal, V.: Different approaches to explore the impact of COVID-19 lockdowns on carbonaceous aerosols at a European rural background site, Science of the Total Environment, 892, https://doi.org/10.1016/j.scitotenv.2023.164527, 2023.

https://doi.org/10.5194/ar-2026-15
Preprint. Discussion started: 13 April 2026

Mitra, S., Chakraborty, A. J., Tareq, A. M., Emran, T. Bin, Nainu, F., Khusro, A., Idris, A. M., Khandaker, M. U., Osman, H., Alhumaydhi, F. A., and Simal-Gandara, J.: Impact of heavy metals on the environment and human health: Novel therapeutic insights to counter the toxicity, J. King Saud Univ. Sci., 34, https://doi.org/10.1016/j.jksus.2022.101865, 2022.

Mukaka, M. M.: Statistics Corner: A guide to appropriate use of Correlation coefficient in medical research, Malawi Medical Journal, 69–71 pp., 2012.

Schober, P. and Schwarte, L. A.: Correlation coefficients: Appropriate use and interpretation, Anesth. Analg., 126, 1763–1768, https://doi.org/10.1213/ANE.0000000000002864, 2018.

Sen, P. K.: Estimates of regression coefficient based on Kendall's tau, J. Am. Stat. Assoc., 63, 324, 1968.

Škáchová, H.: Hodnocení metod stanovení podmínek pro rozptyl znečišťujících látek v období 2007–2018 v Ústeckém kraji, Meteorologické zprávy, 73, 103–109, 2020.

Škáchová, H. and Keder, J.: Nová metodika pro stanovení tříd rozptylových podmínek pomocí ventilačního indexu, Meteorologické zprávy, 78, 21–29, 2025.

Soleimanpour, M., Alizadeh, O., and Sabetghadam, S.: Analysis of diurnal to seasonal variations and trends in air pollution potential in an urban area, Sci. Rep., 13, https://doi.org/10.1038/s41598-023-48420-x, 2023.

Stull, R.: An introduction to boundary layer meteorology, Springer Netherlands, 670 pp., https://doi.org/10.1007/978-94-009-3027-8, 2003.

Stull, R.: Practical Meteorology: An Algebra-based Survey of Atmospheric Science, AVP International, University of British Columbia, 942 pp., 2016.

Suvarapu, Lakshmi Narayana and Baek, Sung-Ok: Determination of heavy metals in the ambient atmosphere: A review, Toxicol. Ind. Health, 33, 79–96, https://doi.org/10.1177/0748233716654827, 2017.

Tchounwou, P. B., Yedjou, C. G., Patlolla, A. K., and Sutton, D. J.: Heavy metal toxicity and the environment, https://doi.org/10.1007/978-3-7643-8340-4_6, 2012.

Theil, H.: A rank invariant method of linear and polynomial regression analysis, i, ii, iii. , Proceedings of the Koninklijke Nederlandse Akademie Wetenschappen, Series A - Mathematical Sciences 53, 53, 386–392, 1950.

Travnikov, O., Batrakova, N., Gusev, A., Ilyin, I., Kleimenov, M., Rozovskaya, O., Shatalov, V., Strijkina, I., Aas, W., Breivik, K., Nizzetto, B., Pfaffhuber, K. A., Mareckova, K., Poupa, S., Wankmueller, R., and Seussall, K.: Assessment of transboundary pollution by toxic substances: Heavy metals and POPs METEOROLOGICAL SYNTHESIZING CENTRE-EAST, 2020.

Venegas, L. E. and Mazzeo, N. A.: Atmospheric stagnation, recirculation and ventilation potential of several sites in Argentina, Atmospheric Research, 43–57 pp., 1999.

Williams, M. L.: Atmospheric Dispersal of Pollutants and the Modelling of Air Pollution, in: Pollution: Causes, Effects and Control, edited by: Harrison, R. M., The Royal Society of Chemistry, 0, https://doi.org/10.1039/BK9781849736480-00225, 2013.

https://doi.org/10.5194/ar-2026-15
Preprint. Discussion started: 13 April 2026

Wu, Y., Liu, B., Meng, H., Dai, Q., Shi, L., Song, S., Feng, Y., and Hopke, P. K.: Changes in source apportioned VOCs during high O3 periods using initial VOC-concentration-dispersion normalized PMF, Science of the Total Environment, 896, https://doi.org/10.1016/j.scitotenv.2023.165182, 2023.

Yang, Y., Liu, B., Hua, J., Yang, T., Dai, Q., Wu, J., Feng, Y., and Hopke, P. K.: Global review of source apportionment of volatile organic compounds based on highly time-resolved data from 2015 to 2021, https://doi.org/10.1016/j.envint.2022.107330, 1 July 2022.

Zhang, Y.: Dynamic effect analysis of meteorological conditions on air pollution: A case study from Beijing, Science of the Total Environment, 684, 178–185, https://doi.org/10.1016/j.scitotenv.2019.05.360, 2019.